

Six years of *BeppoSAX* observations of blazars: A spectral catalog[★]

D. Donato¹, R. M. Sambruna^{1,2}, and M. Gliozzi^{1,2}

¹ George Mason University, School of Computational Sciences, 4400 University Drive, Fairfax, VA 22030, USA
e-mail: davide@physics.gmu.edu

² George Mason University, Dept. Of Physics & Astronomy, MS 3F3, 4400 University Drive, Fairfax, VA 22030, USA

Received 21 October 2003 / Accepted 13 December 2004

Abstract. We present a spectral catalog for blazars based on the *BeppoSAX* archive. The sample includes 44 High-energy peaked BL Lacs (HBLs), 14 Low-energy peaked BL Lacs (LBLs), and 28 Flat Spectrum Radio Quasars (FSRQs). A total of 168 LECS, MECS, and PDS spectra were analyzed, corresponding to observations taken in the period 1996–2002. The 0.1–50 keV continuum of LBLs and FSRQs is generally fitted by a single power law with Galactic column density. A minority of the observations of LBLs (25%) and FSRQs (15%) is best fitted by more complex models like the broken power law or the continuously curved parabola. These latter models provide also the best description for half of the HBL spectra. Complex models are more frequently required for sources with fluxes $F_{2-10 \text{ keV}} > 10^{-11} \text{ erg cm}^{-2} \text{ s}^{-1}$, corresponding to spectra with higher signal-to-noise ratio. As a result, considering sources with flux above this threshold, the percentage of spectra requiring those models increases for all the classes. We note that there is a net separation of X-ray spectral properties between HBLs on one side, and LBLs and FSRQs on the other, the distinction between LBLs and FSRQs is more blurry. This is most likely related to ambiguities in the optical classification of the two classes.

Key words. galaxies: active – galaxies: fundamental parameters – galaxies: nuclei – X-rays: galaxies – catalogs

1. Introduction

Blazars are a class of radio-loud Active Galactic Nuclei (AGN) defined by non-thermal emission from a jet oriented close to the line of sight. Multiwavelength blazar studies have made it clear that their spectral energy distributions (SEDs) are characterized, in a $\nu\text{-}\nu F(\nu)$ plot, by two broad peaks (Giommi & Padovani 1994). The first component, peaking anywhere in the IR-soft X-ray band, is due to synchrotron emission, while the higher-energy one is due to the inverse Compton emission of ambient photons off the same electrons producing the synchrotron part of the spectrum (Maraschi et al. 1992; Sikora et al. 1994; but see Mannheim 1993 for a different interpretation).

Previous studies have shown that low-luminosity BL Lacs (High-energy peaked BL Lacs, or HBLs) exhibit the synchrotron peak in the UV-soft X-ray band, and the inverse Compton peak between the GeV and the TeV band (Sambruna et al. 1994; Giommi et al. 1995; Padovani & Giommi 1995; Fossati et al. 1997). The two components have approximately the same power. For mid-luminosity sources (Low-energy peaked BL Lacs, or LBLs) the synchrotron peak is in the near infrared band and the X-ray emission is due either to the

synchrotron or the Compton component, or both. For the high-luminosity sources (Flat Spectrum Radio Quasars, or FSRQs) the synchrotron peak is in the far infrared band while X-ray emission is ascribed to the Compton component.

The X-ray band, at the overlap of the synchrotron and Compton components, is key to disentangle the contribution of the two components to the broad band continuum. Based on current unification studies (e.g., Fossati et al. 1997) one expects the low-luminosity sources to be dominated by the high-energy tail of the synchrotron emission in the X-rays, and thus to have steep (photon index $\Gamma > 2$, where $F_\nu \propto \nu^{-(\Gamma-1)}$) or convex X-ray spectra, as a result of radiative losses. On the other hands, FSRQs should have flatter spectra ($\Gamma < 2$), while LBLs should exhibit intermediate slopes, or even concave X-ray continua.

Previous systematic analysis of the X-ray continua of blazars relied on satellites with limited sensitivity (e.g., *EXOSAT*; Sambruna et al. 1994a,b) or limited bandpass (*ROSAT*, Urry et al. 1996; Perlman et al. 1996; *ASCA*, Sambruna et al. 1999; Donato et al. 2001). These studies showed that the X-ray spectra of blazars are often complex, with downward-curved continua in HBLs and occasionally upward-curved continua in FSRQs and LBLs.

With its wide X-ray band pass (0.1–200 keV) and good sensitivity, *BeppoSAX* is the instrument of choice to study the broadband X-ray continua of blazars. The *BeppoSAX* mission

[★] Tables 2–5 are only available in electronic form at <http://www.edpsciences.org>

ended in early 2002; during its lifetime, *BeppoSAX* observed a large number of blazars as part of multiwavelength campaigns or to obtain snapshot X-ray spectra. The *BeppoSAX* observations for individual sources were published by the original PIs of the investigation. Here we present a uniform analysis of all the public LECS, MECS, and PDS observations, focusing on the spectral properties. A similar previous account was given by Giommi et al. (2002).

The paper is organized as follows. In Sect. 2 we describe the sample selection, and in Sect. 3 the data reduction. In Sect. 4 the spectral catalog is described, while in Sect. 5 we discuss the results. Throughout this paper, $H_0 = 75 \text{ km s}^{-1} \text{ Mpc}^{-1}$ and $q_0 = 0.5$ are adopted.

2. Sample selection

The *BeppoSAX* satellite carried onboard four Narrow Field Instruments (NFI) pointing in the same direction and covering a very large energy range from 0.1 to 300 keV (Boella et al. 1997). Two of the four instruments have imaging capability, the Low Energy Concentrator Spectrometer (LECS), sensitive in the nominal range 0.1–10 keV, and three Medium Energy Concentrator Spectrometers (MECS), sensitive in the nominal range 1–10 keV. The other two detectors are the High Pressure Proportional Counter (HPGSPC), sensitive in the nominal range 4–120 keV, and the Phoswich Detector System (PDS), sensitive in the nominal range 13–300 keV. We restricted our analysis to the LECS, MECS, and PDS archives, as the HPGSPC has not enough sensitivity to detect relatively faint sources as blazars.

We cross-correlated the *BeppoSAX* database with published lists of blazars, including Fossati et al. (1997), Donato et al. (2001), and Giommi et al. (2002), and references herein. Following Padovani & Giommi (1995), sources with the radio-to-X-ray spectral index, α_{rx} , smaller than 0.75 were classified as HBLs, while sources with $\alpha_{\text{rx}} \geq 0.75$ were classified as LBLs or FSRQs, depending on the EW of the optical emission lines.

The sample is presented in Table 1, where we list the name of the object (Col. 1), the coordinates for the equinox 2000.0 (Cols. 2 and 3), the redshift (Col. 4), the Galactic column density $N_{\text{H}}^{\text{Gal}}$ (Col. 5), and the number of *BeppoSAX* observations of the source (Col. 6). The Galactic column was derived from Dickey & Lockman (1990). The sample includes 86 blazars: 44 HBLs, 14 LBLs, and 28 FSRQs. Most sources were observed as part of multiwavelength campaigns, or in a single snapshot observation to obtain the Spectral Energy Distributions. Since the *BeppoSAX* selection process favored objects known for their high X-ray brightness, the sample is highly heterogeneous (with some sources observed multiple times), strongly biased, and by no means complete.

3. Observations and data analysis

All public observations up to January 2002 were analyzed, for a total of 168 spectra. In Table 2 we present the log of the observations, together with the exposure times and the mean count rates in the various instruments. For each observation we report

Table 1. The sample.

Obj. name	RA(J2000)	Dec(J2000)	Redshift	$N_{\text{H}}^{\text{Gal}}$ 10^{20}	No. of observ.
(1)	(2)	(3)	(4)	(5)	(6)
HBLs					
1ES 0033+595	00 35 52.5	+59 50 03.9	0.086	42.7	
1ES 0120+340	01 23 08.5	+34 20 48.9	0.272	5.14	2
RX J0136.5+3905	01 36 32.8	+39 05 56.0	–	6.01	
1ES 0145+138	01 48 29.8	+14 02 16.0	0.125	5.18	
MS 0158.5+0019	02 01 06.2	+00 34 00.0	0.298	2.67	
1ES 0229+200	02 32 48.4	+20 17 16.0	0.140	9.32	
MS 0317.0+1834	03 19 51.8	+18 45 35.0	0.190	10.4	
1ES 0323+022	03 26 13.9	+02 25 14.9	0.147	8.81	
1ES 0347-121	03 49 23.2	-11 59 27.0	0.185	3.63	
1ES 0414+009	04 16 52.4	+01 05 24.0	0.287	10.5	
1ES 0502+675	05 07 56.2	+67 37 24.0	0.314	9.11	
1ES 0507-040	05 09 38.2	-04 00 46.0	0.304	9.74	
PKS 0548-322	05 50 40.6	-32 16 14.9	0.069	2.20	3
MS 0737.9+7441	07 44 05.2	+74 33 58.0	0.315	3.29	
B20912+29	09 15 52.3	+29 33 20.0	–	1.97	
1ES 0927+500	09 30 37.6	+49 50 26.9	0.188	1.40	
1ES 1028+511	10 31 18.4	+50 53 36.0	0.361	1.15	
RX J1037.7+5711	10 37 44.2	+57 11 54.9	–	0.55	
RX J1058.6+5628	10 58 37.6	+56 28 11.9	0.144	0.68	2
1ES 1101-232	11 03 37.6	-23 29 30.9	0.186	6.05	2
Mkn 421	11 04 27.3	+11 04 27.3	0.030	1.34	16
RX J1117.1+2014	11 17 06.1	+20 14 07.0	0.139	1.33	
1ES 1118+424	11 20 48.0	+42 12 12.0	0.124	1.93	
1ES 1133+704	11 36 26.4	+70 09 28.0	0.045	1.40	
RX J1211.9+2242	12 11 58.0	+22 42 36.0	0.455	2.22	3
ON325	12 17 52.0	+30 07 00.9	0.130	1.70	2
1ES 1218+304	12 21 21.7	+30 10 36.9	0.182	1.71	
1ES 1255+244	12 57 31.9	+24 12 38.9	0.141	1.34	
MS 1312.1-4221	13 15 03.7	-42 36 50.0	0.108	8.45	
1RXS J141756.8+25	14 17 56.7	+25 43 28.9	0.237	1.58	3
1ES 1426+428	14 28 32.5	+42 40 18.9	0.129	1.36	
MS 14588+2249	15 01 02.8	+22 37 54.9	0.235	3.54	
1ES 1517+656	15 17 47.6	+65 25 23.9	0.702	1.93	
1ES 1533+535	15 35 00.7	+53 20 38.0	0.890	1.32	
1ES 1544+820	15 40 15.5	+81 55 04.0	–	4.32	
1ES 1553+113	15 55 43.1	+11 11 20.0	0.360	3.67	
Mkn 501	16 53 52.2	+39 45 37.0	0.034	1.81	11
H1722+119	17 25 04.3	+11 52 15.9	0.018	8.86	
1ES 1741+196	17 43 57.7	+19 35 08.9	0.084	6.68	
1ES 1959+650	19 59 59.8	+65 08 54.9	0.047	9.89	3
PKS 2005-489	20 09 25.3	-48 49 53.0	0.071	5.09	2
PKS 2155-304	21 58 51.7	-30 13 28.9	0.116	1.70	3
1ES 2344+514	23 47 04.8	+51 42 17.9	0.044	15.4	7
H2356-309	23 59 07.6	-30 37 36.9	0.165	1.37	
LBLs					
PKS 0048-09	00 50 41.2	-09 29 05.9	–	3.85	
3C 66A	02 22 39.6	+43 02 08.0	0.444	9.41	2
AO 0235+164	02 38 38.8	+16 36 59.0	0.940	8.85	
PKS 0537-441	05 38 50.3	-44 05 08.9	0.894	3.94	
S50716+71	07 21 53.4	+71 20 35.9	–	3.84	3
OJ287	08 54 49.0	+20 06 32.0	0.306	3.05	2
PKS 1144-379	11 47 01.4	-38 12 11.0	1.048	7.53	
ON231	12 21 31.6	+28 13 58.0	0.102	1.88	2
OQ530	14 19 46.6	+54 23 16.0	0.151	1.18	3
PKS 1519-273	15 22 37.7	-27 30 11.0	0.071	8.41	
S51803+784	18 00 45.7	+78 28 04.0	0.680	3.94	
3C 371	18 06 50.6	+69 49 27.9	0.051	4.74	
4C 56.27	18 24 07.1	+56 51 00.0	0.664	4.14	
BLLAC	22 02 43.3	+42 16 40.0	0.069	20.1	5
FSRQs					
PKS 0208-512	02 10 46.1	-51 01 01.9	0.999	3.09	
NRAO140	03 36 29.8	+32 18 20.0	1.258	15	
PKS 0521-365	05 22 58.0	-36 27 30.9	0.055	3.45	
PMN 0525-3343	05 25 06.2	-33 43 05.0	4.401	2.24	
PKS 0528+134	05 30 56.4	+13 31 55.0	2.060	25.7	8
WGAJ0546.6-6415	05 46 41.8	-64 15 21.9	0.323	4.44	
PKS 0743-006	07 45 54.1	-00 44 17.0	0.994	6.48	
1ES 0836+710	08 41 24.4	+70 53 41.9	2.172	2.78	
RGB J0909+039	09 09 15.8	+03 54 42.1	3.200	3.48	
PKS 1127-14	11 30 07.0	-14 49 27.1	1.187	3.83	
3C 273	12 29 06.7	+02 03 09.0	0.158	1.79	9
3C 279	12 56 11.1	-05 47 22.0	0.536	2.26	5
GB1428+4217	14 30 23.8	+42 04 36.9	4.715	1.38	
GB1508+5714	15 10 02.8	+57 02 44.9	4.301	1.40	2
PKS 1510-089	15 12 50.4	-09 05 59.9	0.360	8.18	

Table 1. continued.

Obj. name	RA(J2000)	Dec(J2000)	Redshift	$N_{\text{H,Gal}}$ 10^{20} cm^{-2}	No. of observ.
(1)	(2)	(3)	(4)	(5)	(6)
RGB J1629+4008	16 29 01.3	+40 07 58.0	0.272	0.84	
IES 1641+399	16 42 58.8	+39 48 37.0	0.593	1.01	
RGB J1722+2436	17 22 41.3	+24 36 19.0	0.175	4.71	
S41745+62	17 46 13.9	+62 26 56.0	3.889	3.43	
S5 2116+81	21 14 01.2	+82 04 47.9	0.084	7.60	2
PKS 2126-158	21 29 12.1	-15 38 41.9	3.268	4.92	
PKS 2134+004	21 36 38.5	+00 41 53.9	1.932	4.48	
PKS 2149-306	21 51 55.3	-30 27 53.9	2.345	2.11	
PKS 2223+210	22 25 37.9	+21 18 06.9	1.959	4.37	
PKS 2223-05	22 25 47.2	-04 57 02.9	1.404	5.65	
H2230+114	22 32 36.4	+11 43 50.9	1.037	5.00	5
PKS 2243-123	22 46 18.1	-12 06 50.0	0.630	4.78	
H2251+158	22 53 57.7	+16 08 53.9	0.859	6.55	

Columns: 1 = object name as found in *BeppoSAX* archive; 2 = Right Ascension (at J2000); 3 = Declination (at J2000); 4 = redshift; 5 = Galactic absorption based on Dickey & Lockman (1990); 6 = number of observations in the *BeppoSAX* archive.

the LECS count rates in the energy range 0.1–2 keV and the MECS count rates in the energy range 2–10 keV. Inspection of the PDS spectra shows that the background usually dominates above 50 keV. Thus, counts were extracted in the energy range 13–50 keV for all sources. However, for the brightest sources reliable counts up to 200 keV were detected. In these cases, spectral fits to the PDS data were performed in the energy range 0.1–200 keV.

In Table 2, we report the PDS count rates for only those sources which were detected at $\geq 3\sigma$ confidence level. Most of the sources are weak at energies greater than 10 keV and only 36 sources are detected (15 HBLs, 4 LBLs, and 17 FSRQs).

We extracted LECS, MECS, and PDS spectra. The data analysis for the LECS and MECS instruments was based on the linearized, cleaned event files obtained from the on-line archive. The spectra were extracted with the FTOOLS package XSELECT (v. 2.2), using extraction regions of radius of 8' and 4' for the LECS and MECS, respectively. In the case of weak sources, we used a radius of 6' and sometimes even 4' to extract the LECS spectra. The LECS and MECS background is low but not uniformly distributed across the detector. For this reason it is better to evaluate the background from blank fields that are available from the SDC public ftp site. Since these background data were taken in regions of the sky with no detected sources and low Galactic absorption, the low energy X-ray counts coming from sources located in regions with high Galactic absorption may be underestimated and/or the intrinsic absorption may be overestimated.

The spectral analysis was performed with XSPEC v.11.2, using the latest available response matrices from the *BeppoSAX* calibration center. The spectra from LECS, MECS, and PDS detectors were rebinned using the channel grouping suggested by the *BeppoSAX* team which was designed to match the detector resolution and sensitivity in an optimal way. The LECS/MECS and MECS/PDS normalization factors (to account for inter-calibration systematics of the instruments)

were left free to vary; normal acceptable values are in the range 0.65–1.0 and 0.77–0.93, respectively (Fiore et al. 1999). Spectral fits were performed in the energy ranges 0.1–2 keV for the LECS, 2–10 keV for the MECS, and 13–200 keV for the PDS where the calibration is best known and the background contribution negligible. The best-fit models were determined using the χ^2 minimization routine. The significance of the fit improvement, when additional free parameters were added, was evaluated using the F-test, assuming as a threshold for significant improvement $P_{\text{F}} = 95\%$. Uncertainties on the fitted parameters are 90% confidence ($\Delta\chi^2 = 2.7$) for one parameter of interest.

The following spectral models were used to fit the *BeppoSAX* spectra:

- (1) a single power law with photon index Γ and column density N_{H} fixed to the Galactic value;
- (2) a single power law with free N_{H} ;
- (3) a broken power law with break energy E_{break} , and photon indices below and above the break Γ_1 and Γ_2 , respectively;
- (4) a continuously curved parabola (Fossati et al. 2000). The latter has the same parameters as model 3), but Γ_1 and Γ_2 are evaluated at 1 keV and 10 keV, respectively.

We used the following procedure. At first, all the spectra were fitted with model (1). When the fit was unsatisfactory, model (2) was used. In several cases, the fitted column density from model (2) was consistent with the Galactic value within the errors. We interpret this result as marginal evidence for continuum curvature; however, in these cases fits with the curved models (3) and (4) did not provide a significant improvement. The observations for which models (1) and (2) provided the best-fit are reported in Table 3.

However, in the case of bright sources, $F_{2-10 \text{ keV}} > 10^{-11} \text{ erg cm}^{-2} \text{ s}^{-1}$, corresponding to spectra with higher signal-to-noise ratio, a curved model was generally found to provide a better description of the *BeppoSAX* spectra than either model (1) or (2). In few cases (6 observations) where the curved model with Galactic absorption did not provide a good description of the spectrum, the absorption was left free to vary. These observations are listed in Table 4. In Table 5 we also list the fits with models (1) and (2) for the same spectra, for future use. As a summary, the last column of Table 2 reports the model that best-fits the individual spectra for each source in the sample.

The choice of the above spectral models is motivated by previous X-ray studies of blazars (e.g., *EXOSAT*, *Ginga*, *ASCA*; Sambruna et al. 1994a; Tashiro et al. 1995; Takahashi et al. 1996; Donato et al. 2001). These authors found that the X-ray continua of high-luminosity blazars are usually well described by a single power law, while at decreasing luminosities curved X-ray continua are often observed. The latter are convex, with $\Gamma_1 < \Gamma_2$, in HBLs and concave, with $\Gamma_1 > \Gamma_2$, in some LBLs and FSRQs. In the brightest HBLs, the broken power law model is inadequate to represent the continuous curvature of the X-ray spectra, and better results are obtained using a continuously curved model (i.e., Fossati et al. 2000 for MKN 421, Tavecchio et al. 2001 for MKN 501).

An independent analysis of the *BeppoSAX* blazar archive was performed by Giommi et al. (2002), who analyzed a total of 157 X-ray spectra of 84 sources (42 HBLs, 12 LBLs, 22 FSRQs, and 4 GigaHertz Peaked Spectrum QSOs). These authors fitted the LECS+MECS+PDS spectra using a single power law, a broken power law, a sum of two power laws, and a logarithmic parabola. For each model the N_{H} was fixed at the Galactic value. Comparing the results for the models that are in common with this work (single power law or broken power law), we find that our results are completely consistent with Giommi et al. (2002).

4. The spectral catalog

The results of our spectral analysis, from fits to the joint LECS+MECS+PDS datasets in the energy range 0.1–200 keV, are reported in Tables 3 and 4. For each source we present the parameters obtained with the model that best-fits the data (power-law model in Table 3 and curved model in Table 4), and their 90% confidence uncertainties. For sources with multiple observations, different models best-fit the data at different epochs. We reported the individual best-fit models, using a different procedure than Giommi et al. 2002, who systematically used the same model for repeatedly observed sources.

For the HBL class we obtained spectral information for 90 observations of 44 sources. For 46 observations (corresponding to 15 sources) the model that best-fits the LECS+MECS+PDS data is a downward-curved model (broken power law or curved parabola), while the remaining observations are described by a single power law. In the latter cases, the photon index is steep, $\Gamma \gtrsim 2$. The energy break, in the cases of a curved model fit, is more frequently located around 1–2 keV. Although for most of the sources the best fit is obtained with intrinsic absorption fixed to the Galactic value, 20 spectral fits corresponding to 17 sources require a column density of the order of 10^{20} cm^{-2} . This may indicate residual curvature in the continuum which the model is still inadequate to describe.

For the LBL class we analyzed 25 observations of 14 sources. For 7 observations (corresponding to 4 sources) the model that best-fits the LECS+MECS+PDS data is a curved model, while the remaining observations are described by a single power law. The photon indices of the single power laws are flat, $\Gamma < 2$, in 9 sources (13 observations) and steep, $\Gamma \geq 2$, in 4 sources (4 observations). For the sources with a spectrum described by a curved model, S5 0716+71 and ON 231 need for all their observations an upward curvature, with a steep photon index below the break ($\Gamma_1 \geq 2.4$) and a flatter index above the break ($\Gamma_2 \leq 2$). One observation of 3C 66A and one of BL Lac need a downward-curved model. In both sources, $\Gamma_1 \sim 2.2$, while $\Gamma_2 \sim 2.3$ and 2.6, respectively, while the break energy is at 0.3–0.4 keV. Among the sources with multiple observations, only BL Lac shows spectral variability, with a total change of the photon index $\Delta\Gamma \sim 1$ for a change of the flux of a factor 3 (from 6 to $20 \times 10^{-12} \text{ erg cm}^{-2} \text{ s}^{-1}$).

Finally, for the FSRQ class 53 observations (corresponding to 28 sources) were analyzed. The best-fit is always obtained using a single power law (model (1)) with $\Gamma \leq 1.8$, except for

1ES 0836+710, PKS 1510-089, PKS 2126-158, and 5 observations of 3C 273, for which a curved model is needed. All the observations are fitted using the intrinsic absorption fixed to the Galactic value. For 1ES 0836+710 and PKS 2126-158 downward curvature is detected, with $\Gamma_1 \sim 1$ and $\Gamma_2 \sim 1.3$ and 1.8, respectively. For 3C 273 and PKS 1510-089 upward curvature is indicated, indicating the presence of a soft excess.

Since the soft excess can have thermal origins (e.g., accretion disk), we fitted the *BeppoSAX* data with a power law plus either a blackbody or a bremsstrahlung. The inclusion of either thermal component was not statistically preferred to a broken power law. Thus, the origin of the soft excess in 3C 273 and PKS 1510-089 is still an open question.

5. Results and discussion

We presented a uniform analysis of the *BeppoSAX* archival spectra for blazars. We will now use the spectral catalog to infer the average X-ray properties of the three blazar classes. While these properties were investigated before with *ASCA* (Sambruna et al. 1999; Donato et al. 2001), only *BeppoSAX* has the unique combination of wide bandpass and sensitivity necessary to study the entire X-ray range. An important caveat, however, is that the “sample” is incomplete and by all means biased toward the brightest X-ray sources of each class.

First, we derive average X-ray spectral parameters for each best-fit model and each class of blazars. To avoid a bias toward sources observed multiple times, we adopted the following procedure. For sources observed only a few times (≤ 9) and with negligible variations in spectral index ($\Delta\Gamma \lesssim 0.5$) or flux variation of a factor of ~ 2 between maximum and minimum, we used the observation for which the spectral parameters are better constrained. For sources observed multiple times and with significant spectral or flux variations, we considered two observations, corresponding to the two most extreme values of the spectral index and/or flux. This procedure yielded 47 observations of 44 HBLs (Mkn 421, Mkn 501, and 1ES 2344+514 were observed in 2 states), 15 observations of 14 LBLs (BL Lac showed variability both in the flux and in the spectral index), and 29 observations of the 28 FSRQs (PKS 0528+134 showed variability in the spectral index). The average parameters are reported in Table 6.

Second, in order to compare in a homogeneous way all the objects, we parameterize the continuum in 0.1–200 keV with a simple power law plus *fixed* and *free* absorption, even for sources whose spectrum was better described by a curved model. Thus, we used the values of the photon index and luminosity from the fits reported in Tables 3 and 5. Using this approach, a convex/concave continuum will be represented by a power law with larger/smaller absorption column than Galactic. To reduce the bias toward sources with multiple observations, we adopted the procedure described above which reduces the number of observations to a maximum of 2 for the most variable sources.

The distributions of the spectral indices from the fits with a single power law model are shown in Fig. 1 for the three classes. Figure 2 shows the distributions for the monochromatic luminosities at 1 keV. The average values are reported in

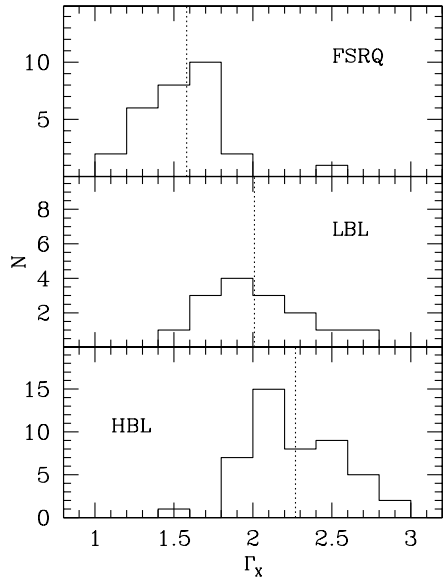


Fig. 1. Distribution of the photon spectral indices obtained using a single power law fit. The dotted line represent the average value reported in Table 7.

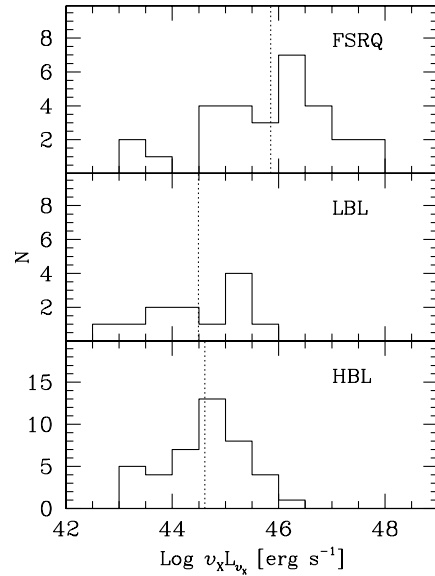


Fig. 2. Distribution of the νL_ν monochromatic (1 keV) luminosity for the three subclasses obtained using a single power law fit. The dotted line is the average spectral index from Table 7.

Table 6. Average spectral parameters for the best-fit models.

	HBL	LBL	FSRQ
a) Single power law			
N	34	12	26
$\langle \Gamma_{PL} \rangle$	2.24(0.04)	1.92(0.07)	1.59(0.05)
b) Broken power law			
N	6	2	2
$\langle \Gamma_1 \rangle$	2.06(0.18)	2.29(0.07)	1.06(0.03)
$\langle E_{break} \rangle$	2.24(1.02)	1.10(0.65)	0.49(0.11)
$\langle \Gamma_2 \rangle$	2.65(0.26)	2.24(0.40)	1.56(0.22)
c) Continuously curved parabola			
N	7	1	1
$\langle \Gamma_1 \rangle$	1.91(0.14)	2.58	2.51
$\langle E_{break} \rangle$	1.71(0.36)	3.10	1.40
$\langle \Gamma_2 \rangle$	2.53(0.12)	1.58	1.32

The break energy is in keV. For each value we report also the standard deviation (in parenthesis) and the number N of observations used.

Table 7. To compare the distributions of the 3 classes in Figs. 1 and 2, we used a Kolmogorov-Smirnov test, which gives the probability P_{KS} that 2 distributions are drawn from the same parent population. Therefore, small values of P_{KS} indicate that the cumulative distribution function of the first data set is significantly different from that of the second data set. For the spectral index distributions in Fig. 1, $P_{KS} \sim 0.23$ for HBLs vs. LBLs, $P_{KS} \sim 0.99$ for HBLs vs. FSRQs, and $P_{KS} \sim 0.83$ for LBLs vs. FSRQs. Thus, we conclude that there is no significant difference in the spectral index distribution among the three classes. However, the Kolmogorov-Smirnov test is sensitive only to the shape of the distribution, and not to the location of its centroid. We thus compared the average values of the

Table 7. Average parameters for the blazar classes.

	HBL	LBL	FSRQ
N	47	15	29
$\langle \Gamma \rangle$	2.27(0.04)	2.01(0.08)	1.58(0.05)
$\langle L_x \rangle$	44.61(0.11)	44.49(0.27)	45.85(0.22)

Average values of the X-ray photon indices and monochromatic 1 keV luminosities from fitting all the *BeppoSAX* spectra with either model (1) or model (2). The standard deviation are in parenthesis.

spectral index for the 3 subclasses in Table 7. Comparing the average indices for HBLs and LBLs and for LBLs and FSRQs we found that they are marginally consistent at 2σ and 3σ , respectively. On the other hand, the average spectral index of HBLs is significantly different from the FSRQs, with HBLs having a steeper X-ray continua than FSRQs.

Similar conclusions are derived if the average luminosities of the three classes are compared. Using the Kolmogorov-Smirnov test, we find $P_{KS} \sim 0.31$ for HBLs vs. LBLs, $P_{KS} \sim 0.89$ for HBLs vs. FSRQs, and $P_{KS} \sim 0.31$ for LBLs vs. FSRQs, suggesting that the distribution shapes are drawn from the same population. Comparing the average luminosities shows that HBLs and FSRQs are different at 3σ , while HBLs and LBLs have similar $\langle L_{1 \text{ keV}} \rangle$.

Using published radio fluxes at 5 GHz, we derived the radio-to-X-ray indices α_{rx} . In Fig. 3 we plot the X-ray photon index from Table 4 versus α_{rx} . The blazars separate in two groups: HBLs have $\alpha_{rx} < 0.75$ and $\Gamma_x > 2$, while LBLs and FSRQs have $\alpha_{rx} > 0.75$ and $\Gamma_x < 2$. One LBL (BL Lac) and 4 FSRQs (WGA J0546.6-6415, RGB J1629+4008, RGB J1722+2436, and S5 2116+81) fill the gap between the two groups. As discussed in Padovani et al. 2002, these sources exhibit spectral energy distributions more similar to HBLs and were dubbed “High-energy peaked

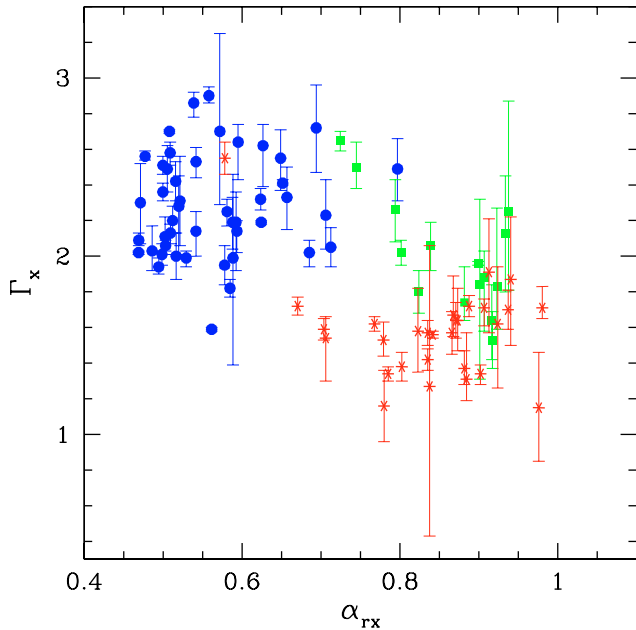


Fig. 3. X-ray photon indices vs. broad band radio to X-ray indexes. Circle: HBLs, square: LBLs, star: FSRQs.

FSRQs”. It still remains to be demonstrated whether the steep soft X-ray spectrum of these sources is due to synchrotron from the jet or is thermal emission perhaps related to the high-energy tail of the disk Blue Bump (as, e.g., in 3C 273).

Figure 4 shows the plot of the radio luminosity versus the X-ray luminosity for HBLs, LBLs, and FSRQs. There is a clear correlation between the luminosities at the two wavelengths. However, different trends are observed between HBLs and LBLs-FSRQs: for a given X-ray luminosity, LBLs and FSRQs appear more luminous at radio.

To quantify the degree of linear correlation, we calculated the linear correlation coefficient r and computed the chance probability $P_r(N)$ that a random sample of N uncorrelated pairs of measurements would yield a linear correlation coefficient equal or larger than $|r|$; if the chance probability is small, the two quantities are likely to be correlated. For HBLs, the linear correlation coefficient is $r = 0.72$ and the chance probability $P_r = 2 \times 10^{-7}$. For LBLs-FSRQs, $r = 0.90$ and $P = 2.8 \times 10^{-15}$. From a linear fit to the data in Fig. 4 (i.e., considering the logarithmic values for the luminosities), we derive the following expressions: $\text{Log } L_X = 12.5 + 0.64 \times \text{Log } L_R$ for HBLs, and $\text{Log } L_X = -3.9 + 1.06 \times \text{Log } L_R$ for LBLs-FSRQs. These results should be taken with caution, since our sample is very likely biased toward brighter X-ray sources.

In closing, we comment on flux and spectral variability. More details can be found in the publications for individual sources from the original PIs of the observations. Several sources in our sample were observed repeatedly with *BeppoSAX*. Inspection of the plots of flux versus spectral index shows that significant flux and spectral variability is present only for the HBL class, with the familiar trend of flatter slope with increasing flux. This confirms previous results based on various X-ray satellites (e.g., Mkn 421 with *ASCA*, Takahashi et al. 1999).

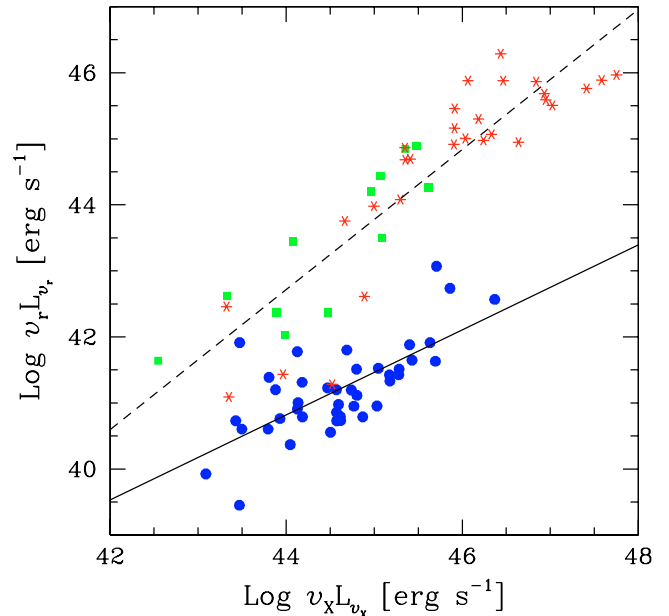


Fig. 4. Monochromatic X-ray (1 keV) luminosities vs. monochromatic radio (5 GHz) luminosities. Circle: HBLs, square: LBLs, star: FSRQs. Linear correlations are plotted for the HBL class (continuous line) and for the LBL-FSRQ classes (dashed line).

In summary, we presented an analysis of the *BeppoSAX* database for blazars. Most HBLs have downward-curved continua, in agreement with the synchrotron interpretation, while the brightest FSRQs and LBLs show upward curvatures. While there is a net separation between HBLs on one side, and LBLs and FSRQs on the other, the distinction between LBLs and FSRQs is more blurry. Conceivably, this is due to optical identification ambiguities, as the classification of a higher-luminosity blazar as an LBL or FSRQ depends on the Equivalent Width of the optical emission lines; thus, variability of the optical continuum makes this classification highly dependent on the observation epoch.

Acknowledgements. We gratefully acknowledge financial support from NASA grants NAG5-10073 (D.D., R.M.S.) and LTSA grant NAG5-10708 (R.M.S., M.G.). R.M.S. was also supported by an NSF CAREER award and the Clare Boothe Luce Program of the Henry Luce Foundation. This research made use of data retrieved from the ASI/ASDC-*BeppoSAX* public archive and the NASA/IPAC Extragalactic Database (NED) which is operated by the Jet Propulsion Laboratory, Caltech, under contract with the National Aeronautics and Space Administration.

References

- Boella, G., Butler, R. C., Perola, G. C., et al. 1997, *A&AS*, 122, 299
- Dickey, J. M., & Lockman, F. J. 1990, *ARA&A*, 28, 215
- Donato, D., Ghisellini, G., Tagliaferri, G., & Fossati, G. 2001, *A&A*, 375, 739
- Fiore, F., Guainazzi, M., & Grandi, P. 1999, *Cookbook for NFI BeppoSAX Spectral Analysis v. 1.2*

- Fossati, G., Maraschi, L., Celotti, A., Comastri, A., & Ghisellini, G. 1997, *MNRAS*, 289, 136
- Fossati, G., Celotti, A., Chiaberge, M., et al. 2000, *ApJ*, 541, 166
- Giommi, P., & Padovani, P. 1994, *MNRAS*, 268, 51
- Giommi, P., Ansari, S. G., & Micol, A. 1995, *A&AS*, 109, 267
- Giommi, P., Capalbi, M., Fiocchi, M., et al. 2002, *Babs. Conf.*, 63
- Mannheim, K. 1993, *A&A*, 269, 67
- Maraschi, L., Ghisellini, G., & Celotti, A. 1992, *ApJ*, 397, L5
- Padovani, P., & Giommi, P. 1995, *ApJ*, 444, 567
- Padovani, P., Costamante, L., Ghisellini, G., Giommi, P., & Perlman, E. 2002, *ApJ*, 581, 895
- Perlman, E. S., Stocke, J. T., Wang, Q. D., & Morris, S. L. 1996, *ApJ*, 456, 451
- Sambruna, R. M., Barr, P., Giommi, P., et al. 1994a, *ApJS*, 95, 371
- Sambruna, R. M., Barr, P., Giommi, P., et al. 1994b, *ApJ*, 434, 468
- Sambruna, R. M., Maraschi, L., & Urry, C. M. 1996, *ApJ*, 463, 444
- Sambruna, R. M., Eracleous, M., & Mushotzky, R. F. 1999, *ApJ*, 526, 60
- Sikora, M., Begelman, M. C., & Rees, M. J. 1994, *ApJ*, 421, 153
- Takahashi, T., Tashiro, M., Madejski, G., et al. 1996, *ApJ*, 470, 89
- Takahashi, T., Madejski, G., & Kubo, H. 1999, *Aph*, 11, 177
- Tashiro, M., Makishima, K., Ohashi, T., et al. 1995, *PASJ*, 47, 131
- Tavecchio, F., Maraschi, L., Pian, E., et al. 2001, *ApJ*, 554, 725
- Urry, C. M., Sambruna, R. M., Worrall, D. M., et al. 1996, *ApJ*, 463, 424

Online Material

Table 2. continued.

Obj. name	Obs. date	Seq. num	LECS	c/s	MECS	c/s	PDS	c/s	Model
(1)	(2)	(3)	(ks)	(10 ⁻²)	(ks)	(10 ⁻²)	(ks)	(10 ⁻²)	(10)
PKS 2005-489	29-Sep.-1996	50046001	0.0	...	9.9	35.95 ± 0.60	7.7	...	1
	01-Nov.-1998	50503002	20.7	167.50 ± 0.91	52.5	201.40 ± 0.62	23.4	66.4 ± 3.0	3
PKS 2155-304	20-Nov.-1996	50016001	36.3	132.30 ± 0.61	106.9	33.28 ± 0.18	43.3	13.1 ± 2.3	4
	22-Nov.-1997	50160008	22.5	189.90 ± 0.93	59.5	104.50 ± 0.42	28.0	9.5 ± 2.8	4
	04-Nov.-1999	50880001	46.1	82.97 ± 0.43	104.0	31.43 ± 0.18	49.1	...	4
1ES 2344+514	03-Dec.-1996	50320001	4.7	9.61 ± 0.47	13.0	8.64 ± 0.26	6.0	...	1
	04-Dec.-1996	50320002	5.3	10.16 ± 0.46	13.2	10.38 ± 0.28	6.1	...	2
	05-Dec.-1996	50320003	3.5	17.09 ± 0.72	8.0	13.89 ± 0.42	3.8	...	1
	07-Dec.-1996	50320004	5.6	16.74 ± 0.57	14.0	18.72 ± 0.37	6.4	29.4 ± 5.9	1
	11-Dec.-1996	50320005	3.0	9.82 ± 0.60	13.0	11.71 ± 0.30	5.8	...	1
	26-Jun.-1998	50760001	13.5	6.26 ± 0.23	50.6	9.75 ± 0.14	21.4	...	1
	03-Dec.-1999	50969001	28.8	5.35 ± 0.14	90.1	10.09 ± 0.11	45.3	...	3
H2356-309	21-Jun.-1998	50493007	15.4	21.33 ± 0.38	41.0	27.64 ± 0.26	18.0	13.4 ± 3.4	3
LBLs									
PKS 0048-09	19-Dec.-1997	500460031	4.7	1.35 ± 0.20	9.9	1.45 ± 0.14	4.3	...	1
3C 66A	31-Jan.-1999	50750003	8.9	3.11 ± 0.20	26.4	2.36 ± 0.11	12.7	...	4
	29-Jul.-2001	51372002	19.8	4.18 ± 0.16	50.2	2.88 ± 0.08	23.1	9.8 ± 2.7	2
AO 0235+164	28-Jan.-1999	50482001	25.0	0.47 ± 0.07	29.2	0.87 ± 0.07	25.8	...	1
PKS 0537-441	28-Nov.-1998	50497002	24.1	1.71 ± 0.10	47.4	2.44 ± 0.08	36.7	...	1
S 50716+71	14-Nov.-1996	50160001	16.9	2.23 ± 0.13	122.5	0.75 ± 0.03	47.2	...	3
	07-Nov.-1998	50750002	9.5	2.39 ± 0.18	31.3	2.86 ± 0.13	16.2	11.5 ± 3.5	4
	30-Oct.-2000	51153001	19.2	3.77 ± 0.15	43.5	3.31 ± 0.09	22.4	...	3
OJ287	24-Nov.-1997	50046002	5.2	0.72 ± 0.15	10.7	2.58 ± 0.17	4.5	...	1
	20-Nov.-2001	51336001	23.8	0.58 ± 0.07	39.8	1.40 ± 0.07	26.9	...	1
PKS 1144-379	10-Jan.-1997	50046006	10.8	0.84 ± 0.11	23.2	0.43 ± 0.05	9.8	...	1
ON231	11-May-1998	50503001	21.1	8.01 ± 0.20	24.9	4.14 ± 0.14	11.6	15.8 ± 4.3	3
	11-Jun.-1998	505030011	17.6	5.63 ± 0.21	31.8	3.24 ± 0.11	16.6	14.1 ± 3.6	3
OQ530	12-Feb.-1999	50482003	17.8	0.69 ± 0.08	39.7	0.67 ± 0.06	19.2	...	1
	03-Mar.-2000	50881003	19.6	0.83 ± 0.08	26.6	1.15 ± 0.08	10.3	...	1
	26-Mar.-2000	508810031	17.2	0.72 ± 0.09	22.7	0.95 ± 0.08	10.4	...	1
PKS 1519-273	01-Feb.-1998	50046007	9.4	0.78 ± 0.12	26.9	0.66 ± 0.07	12.2	...	1
S51803+784	28-Sep.-1998	50482004	18.7	0.77 ± 0.09	40.5	2.10 ± 0.08	16.4	...	1
3C 371	22-Sep.-1998	50482002	13.3	0.96 ± 0.10	33.9	1.90 ± 0.09	15.1	...	1
4C 56.27	11-Oct.-1997	50046005	4.2	0.93 ± 0.19	13.4	1.15 ± 0.11	59.8	...	1
BLLAC	08-Nov.-1997	50046004	12.5	4.63 ± 0.21	13.8	10.97 ± 0.29	8.3	19.0 ± 5.1	2
	05-Jun.-1999	50881001	45.3	3.94 ± 0.10	54.4	7.13 ± 0.12	26.9	12.1 ± 2.7	1
	05-Dec.-1999	50881002	17.5	3.52 ± 0.15	54.7	12.84 ± 0.16	24.2	11.3 ± 2.7	1
	26-Jul.-2000	51165001	16.9	2.20 ± 0.13	23.3	5.82 ± 0.17	10.4	...	1
	31-Oct.-2000	511650011	24.9	18.23 ± 0.28	33.7	23.90 ± 0.27	18.8	...	4
FSRQs									
PKS 0208-512	14-Jan.-2001	51220002	15.9	1.55 ± 0.12	34.3	4.92 ± 0.13	15.3	13.7 ± 3.3	1
NRAO140	05-Aug.-1999	50997001	17.5	1.83 ± 0.12	50.0	7.36 ± 0.13	22.9	15.2 ± 4.7	1
PKS 0521-365	02-Oct.-1998	50497001	18.0	4.86 ± 0.18	41.1	9.36 ± 0.16	19.1	...	1
PMN 0525-3343	27-Feb.-2000	50849001	24.8	0.45 ± 0.06	59.8	0.79 ± 0.05	28.9	...	1
PKS 0528+134	21-Feb.-1997	50237001	6.3	0.49 ± 0.13	14.4	1.08 ± 0.09	6.6	...	1
	22-Feb.-1997	50237002	5.0	...	13.3	1.22 ± 0.10	5.8	...	1
	27-Feb.-1997	50237003	4.4	...	7.3	0.90 ± 0.12	3.0	...	1
	01-Mar.-1997	50237004	4.3	...	13.5	1.14 ± 0.10	6.1	...	1
	03-Mar.-1997	50237005	5.1	...	14.1	0.91 ± 0.09	6.5	...	1
	04-Mar.-1997	50237006	2.8	...	11.2	1.26 ± 0.11	4.9	...	1
	06-Mar.-1997	50237007	3.1	...	12.7	1.25 ± 0.11	5.5	19.8 ± 6.5	1
	11-Mar.-1997	50237008	2.5	...	11.5	1.05 ± 0.10	5.3	26.6 ± 7.0	1
WGAJ0546.6-6415	01-Oct.-1998	50769002	18.9	2.74 ± 0.13	47.3	8.65 ± 0.14	20.0	14.7 ± 3.2	1
PKS 0743-006	08-May-2001	51143002	10.7	0.48 ± 0.10	36.0	0.93 ± 0.07	16.2	17.8 ± 3.2	1
1ES 0836+710	27-May-1998	50497003	18.5	6.66 ± 0.20	42.6	25.68 ± 0.25	16.5	39.8 ± 3.6	4
RX J0909+0354	27-Nov.-1997	50127002	10.4	0.65 ± 0.11	29.7	1.76 ± 0.09	13.8	14.5 ± 4.0	1
PKS 1127-14	04-Jun.-1999	50850001	18.7	2.80 ± 0.14	47.9	8.77 ± 0.14	22.5	21.0 ± 2.9	1
3C 273	18-Jul.-1996	50021001	11.8	31.79 ± 0.53	129.9	35.30 ± 0.16	60.6	83.1 ± 2.0	3
	13-Jan.-1997	50237011	13.6	55.47 ± 0.65	25.1	58.97 ± 0.48	11.4	147.1 ± 4.7	1
	15-Jan.-1997	50237012	13.3	51.86 ± 0.63	24.0	56.80 ± 0.49	10.8	144.9 ± 4.9	1
	17-Jan.-1997	50237013	12.5	49.68 ± 0.64	27.3	55.10 ± 0.45	12.5	130.8 ± 4.4	1
	22-Jan.-1997	50237014	8.8	48.90 ± 0.76	22.3	51.56 ± 0.48	9.3	130.4 ± 5.1	1
	24-Jun.-1998	50795004	27.9	54.87 ± 0.45	72.2	111.00 ± 0.39	33.8	127.3 ± 2.6	3
	09-Jan.-2000	50795008	34.8	58.20 ± 0.41	85.2	119.70 ± 0.38	42.2	135.1 ± 2.2	3
	13-Jun.-2000	50795010	29.6	44.48 ± 0.39	68.1	89.55 ± 0.36	31.9	93.5 ± 2.3	3
	12-Jun.-2001	50795011	16.9	57.99 ± 0.59	38.4	104.80 ± 0.52	18.5	122.7 ± 3.1	3
3C 279	13-Jan.-1997	50237016	7.4	3.62 ± 0.24	21.8	2.70 ± 0.12	9.0	...	1
	15-Jan.-1997	50237017	8.4	3.46 ± 0.22	23.9	2.85 ± 0.11	10.0	...	1
	18-Jan.-1997	50237018	0.5	...	2.6	2.88 ± 0.35	1.0	...	1
	21-Jan.-1997	50237019	4.2	3.47 ± 0.31	11.7	3.23 ± 0.17	5.1	...	1
	23-Jan.-1997	50237020	11.2	3.42 ± 0.19	24.7	2.78 ± 0.11	11.4	...	1
GB1428+4217	04-Feb.-1999	50508001	27.9	1.10 ± 0.08	90.5	2.67 ± 0.06	46.0	14.8 ± 2.1	1

Table 2. continued.

Obj. name	Obs. date	Seq. num	LECS	c/s	MECS	c/s	PDS	c/s	Model
(1)	(2)	(3)	(ks)	(10^{-2})	(ks)	(10^{-2})	(ks)	(10^{-2})	(10)
GB1508+5714	29-Mar.-1997	50127001	4.3	...	8.8	0.75 ± 0.11	3.9	...	1
	01-Feb.-1998	501270011	7.0	...	17.5	0.51 ± 0.08	7.8	...	1
PKS 1510-089	03-Aug.-1998	50497004	16.2	1.79 ± 0.12	43.9	4.99 ± 0.11	19.4	17.3 ± 3.3	3
RGB J1629+4008	11-Aug.-1999	50869001	21.2	3.28 ± 0.14	44.9	1.40 ± 0.07	22.8	...	1
1ES 1641+399	19-Feb.-1999	50727002	11.1	3.30 ± 0.19	25.9	5.08 ± 0.15	13.1	13.0 ± 3.8	1
RGB J1722+2436	13-Feb.-2000	50869002	12.4	0.71 ± 0.10	44.1	1.08 ± 0.06	19.7	...	1
S41745+62	29-Mar.-1997	50127006	58.4	0.41 ± 0.04	143.0	0.71 ± 0.03	59.8	...	1
S52116+81	29-Apr.-1998	50769001	13.4	7.54 ± 0.25	28.9	16.71 ± 0.24	13.3	15.9 ± 4.0	1
	12-Oct.-1998	507690011	5.7	5.68 ± 0.33	19.7	11.88 ± 0.25	10.5	13.7 ± 4.5	1
PKS 2126-158	24-May.-1999	51003001	79.9	3.62 ± 0.07	108.0	11.07 ± 0.10	51.6	10.5 ± 2.0	4
PKS 2134+004	25-Nov.-2000	51143001	25.9	1.52 ± 0.09	75.1	2.14 ± 0.06	33.1	...	1
PKS 2149-306	31-Oct.-1997	50264001	17.9	2.74 ± 0.14	39.4	7.46 ± 0.15	16.7	13.0 ± 3.7	1
PKS 2223+210	12-Nov.-1997	50127003	14.2	0.81 ± 0.10	18.4	2.09 ± 0.12	10.8	...	1
PKS 2223-05	10-Nov.-1997	50181006	9.4	0.79 ± 0.12	16.2	1.32 ± 0.11	6.9	...	1
H2230+114	11-Nov.-1997	50237021	11.0	2.03 ± 0.15	23.8	5.45 ± 0.16	11.6	...	1
	13-Nov.-1997	50237022	10.3	2.91 ± 0.19	22.3	5.92 ± 0.17	10.2	...	1
	16-Nov.-1997	50237023	13.2	1.91 ± 0.14	25.7	5.84 ± 0.16	12.1	13.7 ± 4.3	1
	18-Nov.-1997	50237024	7.0	2.12 ± 0.20	12.2	5.63 ± 0.22	5.4	...	1
	21-Nov.-1997	50237025	9.5	2.49 ± 0.18	19.4	5.98 ± 0.18	8.6	...	1
PKS 2243-123	18-Nov.-1998	50727005	10.2	1.32 ± 0.14	27.5	1.89 ± 0.09	13.2	...	1
H2251+158	05-Jun.-2000	51220001	17.7	2.94 ± 0.14	48.5	10.92 ± 0.15	22.4	20.3 ± 2.8	1

Columns: 1 = object name; 2 = observation date; 3 = sequence number of the observation; 4 = exposure time for LECS; 5 = counts rate for LECS in the energy range 0.1–2 keV; 6 = exposure time for MECS (for the observations made before May 1997, MECS2 count-rates are considered); 7 = counts rate for MECS in the energy range 2–10 keV; 8 = exposure time for PDS; 9 = counts rate for PDS in the energy range 13–50 keV. Less than 3σ detections are omitted; 10 = model used for the best fit: 1 = power law with absorption fixed at Galactic value; 2 = power law with free absorption; 3 = broken power law with absorption fixed at Galactic value; 4 = continuously curved parabola with absorption fixed at Galactic value; 5 = broken power law with free absorption; 6 = continuously curved parabola with free absorption.

Table 3. Sources with power law as best-fit model.

Obj. name (1)	Obs. date (2)	N_{H} FIXED		N_{H} FREE			Flux (8)
		Γ (3)	$\chi^2_r/\text{d.o.f.}$ (4)	N_{H} (5)	Γ (6)	$\chi^2_r/\text{d.o.f.}$ (7)	
HBLs							
1ES 0033+595	18-Dec.-1999			35.5 ^{+8.3} _{-7.6}	2.06 ^{+0.03} _{-0.03}	1.22/155	58.9
1ES 0120+340	03-Jan.-1999			9.3 ^{+3.3} _{-2.4}	2.13 ^{+0.06} _{-0.05}	1.07/99	17.1
	02-Feb.-1999			5.6 ^{+6.5} _{-2.5}	2.33 ^{+0.09} _{-0.08}	0.84/39	13.3
RX J0136.5+3905	09-Jan.-2001			7.9 ^{+3.3} _{-2.5}	2.58 ^{+0.07} _{-0.06}	1.27/99	10.8
1ES 0145+138	30-Dec.-1997	1.99 ^{+0.60} _{-0.47}	0.91/24				0.6
MS 0158.5+0019	16-Aug.-1996	2.28 ^{+0.27} _{-0.17}	0.86/25				2.9
1ES 0229+200	16-Jul.-2001			10.0 ^{+5.1} _{-4.1}	1.99 ^{+0.05} _{-0.04}	1.03/99	14.9
MS 0317.0+1834	15-Jan.-1997	2.00 ^{+0.13} _{-0.13}	0.98/59				7.1
1ES 0323+022	20-Jan.-1998	2.19 ^{+0.27} _{-0.17}	0.60/32				3.5
1ES 0347-121	10-Jan.-1997	2.03 ^{+0.11} _{-0.14}	1.04/54				6.2
1ES 0414+009	21-Sep.-1996	2.53 ^{+0.09} _{-0.08}	0.94/54				8.7
1ES 0502+675	06-Oct.-1996	2.30 ^{+0.23} _{-0.22}	1.13/97				19.2
1ES 0507-040	11-Feb.-1999	2.14 ^{+0.14} _{-0.11}	0.78/36				5.9
PKS 0548-322	26-Feb.-1999	2.28 ^{+0.43} _{-0.22}	0.61/16				17.8
	07-Apr.-1999			3.1 ^{+0.8} _{-0.8}	2.25 ^{+0.08} _{-0.07}	0.92/35	15.7
MS0737.9+7441	29-Oct.-1996			27.3 ^{+53.5} _{-18.0}	2.70 ^{+0.41} _{-0.55}	0.95/16	1.4
B20912+29	14-Nov.-1997	2.05 ^{+0.11} _{-0.11}	1.01/23				2.8
1ES 0927+500	25-Nov.-1998			3.3 ^{+1.5} _{-1.1}	2.11 ^{+0.10} _{-0.11}	0.96/33	6.8
1ES 1028+511	01-May-1997			4.7 ^{+1.5} _{-1.3}	2.42 ^{+0.11} _{-0.11}	0.91/91	10.1
RX J1037.7+5711	02-Dec.-1998	2.23 ^{+0.19} _{-0.20}	0.94/24				0.9
RX J1058.6+5628	21-May-1998	2.26 ^{+0.60} _{-0.54}	1.08/21				0.3
	23-Nov.-1998			2.3 ^{+1.3} _{-0.8}	2.72 ^{+0.25} _{-0.24}	0.79/33	1.7
1ES 1118+424	01-May-1997	2.19 ^{+0.15} _{-0.14}	0.90/38				3.1
1ES 1133+704	10-Dec.-1996			2.0 ^{+0.9} _{-0.8}	2.55 ^{+0.18} _{-0.16}	0.85/39	5.0
RX J1211.9+2242	27-Dec.-1999	1.93 ^{+0.10} _{-0.10}	1.35/24				2.5
	28-Dec.-2001	1.93 ^{+0.06} _{-0.06}	1.04/90				7.6
	11-Jan.-2002	2.05 ^{+0.12} _{-0.12}	1.00/40				5.6
ON325	23-Dec.-1998	2.55 ^{+0.31} _{-0.27}	1.32/25				0.6
	10-Jan.-2002	2.49 ^{+0.18} _{-0.17}	0.90/33				0.6
1ES 1255+244	20-Jun.-1998	1.95 ^{+0.11} _{-0.11}	0.79/24				11.7
MS 1312.1-4221	21-Feb.-1997	2.31 ^{+0.25} _{-0.25}	0.80/16				4.6
1RXS J141756.8+25	27-Jul.-2000			2.3 ^{+0.8} _{-0.7}	2.20 ^{+0.07} _{-0.08}	1.27/96	9.3
1ES 1426+428	08-Feb.-1999			0.8 ^{+0.4} _{-0.4}	1.94 ^{+0.04} _{-0.05}	1.12/142	20.3
MS 14588+2249	19-Feb.-2001	2.62 ^{+0.23} _{-0.12}	1.24/24				0.7
1ES 1533+535	13-Feb.-1999	2.14 ^{+0.12} _{-0.06}	1.22/69				2.6
1ES 1544+820	13-Feb.-1999	2.64 ^{+0.21} _{-0.10}	0.93/39				1.5
1ES 1741+196	26-Sep.-1998	2.02 ^{+0.08} _{-0.07}	1.14/35				6.9
PKS 2005-489	29-Sep.-1996	2.36 ^{+0.05} _{-0.05}	1.06/118				58.7
1ES 2344+514	03-Dec.-1996	2.05 ^{+0.09} _{-0.08}	0.93/39				17.2
	04-Dec.-1996			13.3 ^{+6.8} _{-6.0}	2.05 ^{+0.08} _{-0.09}	1.10/134	18.8
	05-Dec.-1996	2.12 ^{+0.09} _{-0.08}	1.59/51				27.1
	07-Dec.-1996	1.82 ^{+0.05} _{-0.05}	0.96/230				35.3
	11-Dec.-1996	2.17 ^{+0.03} _{-0.03}	1.15/144				20.4
	26-Jun.-1998	2.32 ^{+0.06} _{-0.06}	0.98/93				8.5
LBLs							
PKS 0048-09	19-Dec.-1997	1.96 ^{+0.01} _{-0.01}	1.11/13				1.4
3C 66A	29-Jul.-2001			14.4 ^{+7.6} _{-7.4}	2.40 ^{+0.15} _{-0.13}	1.49/34	2.7
AO 0235+164	28-Jan.-1999	2.13 ^{+0.33} _{-0.32}	1.15/26				0.7
PKS 0537-441	28-Nov.-1998	1.80 ^{+0.12} _{-0.12}	0.66/24				2.4
OJ287	24-Nov.-1997	1.95 ^{+0.30} _{-0.29}	0.88/24				2.4
	20-Nov.-2001	1.64 ^{+0.22} _{-0.20}	0.93/51				1.3
PKS 1144-379	10-Jan.-1997	1.83 ^{+0.24} _{-0.44}	0.88/26				1.1
OQ530	12-Feb.-1999	1.92 ^{+0.29} _{-0.29}	0.86/26				0.6
	03-Mar.-2000	1.53 ^{+0.29} _{-0.32}	1.06/39				1.1
	26-Mar.-2000	1.88 ^{+0.30} _{-0.15}	0.83/32				0.8
PKS 1519-273	01-Feb.-1998	2.25 ^{+0.44} _{-0.62}	1.46/16				0.5
S51803+784	28-Sep.-1998	1.53 ^{+0.16} _{-0.16}	1.04/22				2.2
3C 371	22-Sep.-1998	1.74 ^{+0.10} _{-0.20}	1.14/51				1.7
4C 56.27	11-Oct.-1997	1.84 ^{+0.53} _{-0.48}	0.97/20				1.1

Table 3. continued.

Obj. name (1)	Obs. date (2)	N_{H} FIXED		N_{H} FREE			Flux (8)
		Γ (3)	$\chi^2/\text{d.o.f.}$ (4)	N_{H} (5)	Γ (6)	$\chi^2/\text{d.o.f.}$ (7)	
BLLAC	08-Nov.-1997			$11.0^{+8.4}_{-6.9}$	$1.88^{+0.06}_{-0.12}$	1.11/33	11.1
	05-Jun.-1999	$2.02^{+0.07}_{-0.07}$	1.12/93				6.5
	05-Dec.-1999	$1.59^{+0.05}_{-0.05}$	0.99/93				12.7
	26-Jul.-2000	$1.88^{+0.12}_{-0.12}$	1.21/24				5.8
FSRQs							
PKS 0208-512	14-Jan.-2001	$1.64^{+0.10}_{-0.10}$	1.33/93				4.5
NRAO140	05-Aug.-1999	$1.57^{+0.07}_{-0.07}$	1.26/93				7.2
PKS 0521-365	02-Oct.-1998	$1.72^{+0.06}_{-0.06}$	1.00/147				8.7
PMN 0525-3343	27-Feb.-2000	$1.58^{+0.23}_{-0.24}$	0.99/52				0.7
PKS 0528+134	21-Feb.-1997	$1.28^{+0.26}_{-0.26}$	0.94/27				2.7
	22-Feb.-1997	$1.26^{+0.28}_{-0.30}$	0.45/24				2.9
	27-Feb.-1997	$1.40^{+0.55}_{-0.57}$	0.94/14				2.1
	01-Mar.-1997	$1.34^{+0.29}_{-0.29}$	1.14/25				3.3
	03-Mar.-1997	$1.15^{+0.30}_{-0.31}$	1.25/24				1.9
	04-Mar.-1997	$1.28^{+0.33}_{-0.34}$	0.76/20				2.6
	06-Mar.-1997	$1.12^{+0.26}_{-0.26}$	1.09/23				2.9
	11-Mar.-1997	$1.62^{+0.36}_{-0.32}$	1.48/21				2.2
WGJ0546.6-6415	01-Oct.-1998	$1.59^{+0.06}_{-0.06}$	1.87/93				8.2
PKS 0743-006	08-May-2001	$1.91^{+0.34}_{-0.30}$	0.81/35				0.9
RGB J0909+039	27-Nov.-1997	$1.16^{+0.20}_{-0.20}$	0.73/42				1.9
PKS 1127-14	04-Jun.-1999	$1.42^{+0.06}_{-0.06}$	0.94/93				8.7
3C 273	13-Jan.-1997	$1.56^{+0.02}_{-0.02}$	0.91/231				117.0
	15-Jan.-1997	$1.58^{+0.02}_{-0.02}$	1.19/231				112.0
	17-Jan.-1997	$1.62^{+0.02}_{-0.02}$	1.35/231				108.0
	22-Jan.-1997	$1.55^{+0.02}_{-0.02}$	0.97/231				103.0
3C 279	13-Jan.-1997	$1.67^{+0.12}_{-0.12}$	0.98/39				5.6
	15-Jan.-1997	$1.70^{+0.11}_{-0.11}$	0.75/50				5.8
	18-Jan.-1997	$1.43^{+0.47}_{-0.47}$	1.00/13				7.4
	21-Jan.-1997	$1.53^{+0.16}_{-0.16}$	0.79/48				6.4
	23-Jan.-1997	$1.59^{+0.10}_{-0.10}$	1.18/50				5.7
GB1428+4217	04-Feb.-1999	$1.53^{+0.09}_{-0.10}$	1.15/35				2.8
GB1508+5714	29-Mar.-1997	$0.65^{+0.83}_{-0.85}$	0.84/14				1.3
	01-Feb.-1998	$1.27^{+0.84}_{-0.79}$	1.33/18				0.5
RGB J1629+4008	11-Aug.-1999	$2.55^{+0.09}_{-0.09}$	1.19/35				1.3
IES 1641+399	19-Feb.-1999	$1.71^{+0.10}_{-0.05}$	1.92/35				5.1
RGB J1722+2436	13-Feb.-2000	$1.54^{+0.24}_{-0.12}$	1.00/44				1.0
S41745+62	29-Mar.-1997	$1.64^{+0.17}_{-0.18}$	0.94/97				0.8
S52116+81	29-Apr.-1998	$1.72^{+0.05}_{-0.05}$	1.23/93				15.8
	12-Oct.-1998	$1.83^{+0.09}_{-0.09}$	1.25/35				11.9
PKS 2134+004	25-Nov.-2000	$1.71^{+0.06}_{-0.12}$	1.69/22				2.2
PKS 2149-306	31-Oct.-1997	$1.38^{+0.08}_{-0.08}$	1.13/32				8.1
PKS 2223+210	12-Nov.-1997	$1.31^{+0.12}_{-0.26}$	0.87/37				2.2
PKS 2223-05	10-Nov.-1997	$1.87^{+0.37}_{-0.35}$	1.17/15				1.3
H2230+114	11-Nov.-1997	$1.57^{+0.12}_{-0.12}$	0.87/35				5.6
	13-Nov.-1997	$1.50^{+0.11}_{-0.11}$	0.95/35				6.2
	16-Nov.-1997	$1.47^{+0.11}_{-0.10}$	0.97/35				6.2
	18-Nov.-1997	$1.49^{+0.17}_{-0.16}$	1.27/41				5.5
	21-Nov.-1997	$1.50^{+0.13}_{-0.13}$	1.16/35				6.2
PKS 2243-123	18-Nov.-1998	$1.67^{+0.12}_{-0.22}$	0.97/44				1.8
H2251+158	05-Jun.-2000	$1.34^{+0.06}_{-0.05}$	1.31/93				11.2

Columns: 1 = object name; 2 = observation date; 3 = photon spectral index; 4 = reduced χ^2 with degrees of freedom. Columns 3 and 4 refer to fits obtained with intrinsic absorption fixed to the Galactic value; 5 = intrinsic absorption (in units of 10^{20} cm^{-2}); 6 = photon spectral index; 7 = reduced χ^2 with degrees of freedom. Columns 5 to 7 refer to fits obtained with intrinsic absorption free to vary; 8 = X-ray unabsorbed flux in the energy range 2–10 keV (in units of $10^{-12} \text{ erg cm}^{-2} \text{ s}^{-1}$).

Table 4. continued.

Obj. name (1)	Obs. date (2)	N_{H} FIXED				N_{H} FREE					Flux (12)
		$\chi^2/\text{d.o.f.}$ (3)	Γ_1 (4)	E_{break} (5)	Γ_2 (6)	$\chi^2/\text{d.o.f.}$ (7)	N_{H} (8)	Γ_1 (9)	E_{break} (10)	Γ_2 (11)	
LBLs											
3C 66A	31-Jan.-1999	1.31/33	$2.20^{+0.12}_{-0.27}$	$0.26^{+1.54}_{-1.07}$	$2.32^{+0.15}_{-0.15}$						2.2
S50716+71	14-Nov.-1996	1.07/48	$2.70^{+0.13}_{-0.14}$	$2.35^{+0.80}_{-1.23}$	$1.96^{+0.16}_{-0.22}$						1.5
	07-Nov.-1998	1.92/33	$2.36^{+0.22}_{-0.37}$	$1.75^{+3.99}_{-1.75}$	$1.84^{+0.26}_{-0.85}$						2.7
ON231	30-Oct.-2000	0.98/33	$2.82^{+0.11}_{-0.12}$	$2.73^{+0.42}_{-1.49}$	$1.78^{+0.23}_{-0.30}$						3.3
	11-May-1998	1.19/33	$2.58^{+0.06}_{-0.06}$	$3.09^{+1.03}_{-1.38}$	$1.58^{+0.28}_{-0.44}$						4.2
BLLAC	11-Jun.-1998	0.87/31	$2.58^{+0.23}_{-0.09}$	$2.70^{+0.47}_{-1.33}$	$1.49^{+0.19}_{-0.22}$						3.4
	31-Oct.-2000	1.29/146	$2.21^{+0.12}_{-0.13}$	$0.45^{+0.39}_{-0.44}$	$2.64^{+0.05}_{-0.05}$						20.2
FSRQs											
1ES 0836+710	27-May-1998	1.14/146	$1.08^{+0.15}_{-0.23}$	$0.38^{+0.37}_{-0.37}$	$1.34^{+0.04}_{-0.02}$						26.3
3C 273	18-Jul.-1996	1.10/229	$2.12^{+0.83}_{-1.19}$	$0.37^{+0.38}_{-0.07}$	$1.58^{+0.01}_{-0.01}$						70.1
	24-Jun.-1998	1.22/146	$1.97^{+0.09}_{-0.06}$	$0.72^{+0.11}_{-0.13}$	$1.61^{+0.02}_{-0.01}$						108.0
	09-Jan.-2000	1.13/146	$1.90^{+0.07}_{-0.05}$	$0.84^{+0.22}_{-0.16}$	$1.63^{+0.01}_{-0.01}$						116.0
	13-Jun.-2000	0.98/146	$2.07^{+0.23}_{-0.12}$	$0.58^{+0.20}_{-0.15}$	$1.64^{+0.02}_{-0.01}$						86.7
PKS 1510-089	12-Jun.-2001	1.06/146	$2.21^{+0.08}_{-0.07}$	$0.82^{+0.11}_{-0.06}$	$1.65^{+0.02}_{-0.02}$						101.0
	03-Aug.-1998	0.80/32	$2.51^{+0.30}_{-0.30}$	$1.41^{+1.21}_{-0.25}$	$1.32^{+0.10}_{-0.10}$						5.5
PKS 2126-158	24-May-1999	0.98/146	$1.03^{+0.12}_{-0.12}$	$0.60^{+6.66}_{-0.58}$	$1.78^{+0.27}_{-0.11}$						10.7

Columns: 1 = object name; 2 = observation date; 3 = reduced χ^2 and degrees of freedom; 4 = first photon spectral index; 5 = energy break in keV; 6 = second photon spectral index. Columns 3 to 6 refer to fits obtained using the broken power law or the continuously curved parabola model with intrinsic absorption fixed to the Galactic value; 7 = reduced χ^2 and degrees of freedom; 8 = intrinsic absorption; 9 = first photon spectral index; 10 = energy break in keV; 11 = second photon spectral index. Columns 7 to 11 refer to fits obtained using the broken power law or the continuously curved parabola model with intrinsic absorption free to vary. The intrinsic absorption is in units of 10^{20} cm^{-2} ; 12 = X-ray unabsorbed flux in the energy range 2–10 keV (in units of $10^{-12} \text{ erg cm}^{-2} \text{ s}^{-1}$).

Table 5. Single power law fits for Spectra in Table 4.

Obj. name (1)	Obs. date (2)	χ^2_r /d.o.f. (3)	N_H (4)	Γ (5)
HBLs				
PKS 0548-322	20-Feb.-1999	1.29/95	$3.2^{+0.8}_{-0.6}$	$2.12^{+0.07}_{-0.06}$
1ES 1101-232	04-Jan.-1997	0.97/257	$2.4^{+2.0}_{-2.0}$	$2.01^{+0.06}_{-0.06}$
	19-Jun.-1998	1.19/92	$3.5^{+2.4}_{-2.4}$	$2.25^{+0.05}_{-0.05}$
Mkn 421	29-Apr.-1997	2.28/239	$2.5^{+1.6}_{-2.5}$	$2.65^{+0.02}_{-0.02}$
	30-Apr.-1997	2.07/239	$2.6^{+2.6}_{-2.6}$	$2.67^{+0.02}_{-0.02}$
	01-May-1997	2.38/239	$2.4^{+2.4}_{-2.4}$	$2.63^{+0.02}_{-0.02}$
	02-May-1997	1.81/239	$2.7^{+0.1}_{-0.2}$	$2.68^{+0.01}_{-0.04}$
	03-May-1997	1.62/239	$2.4^{+0.2}_{-0.2}$	$2.74^{+0.03}_{-0.04}$
	04-May-1997	1.45/239	$2.6^{+0.2}_{-0.1}$	$2.90^{+0.04}_{-0.05}$
	05-May-1997	1.79/239	$2.5^{+0.2}_{-0.2}$	$2.78^{+0.03}_{-0.03}$
	07-May-1997	1.14/46	$1.1^{+0.2}_{-0.1}$	$2.42^{+0.06}_{-0.05}$
	21-Apr.-1998	7.82/155	$2.0^{+0.1}_{-0.1}$	$2.51^{+0.01}_{-0.01}$
	23-Apr.-1998	8.41/155	$1.9^{+0.1}_{-0.1}$	$2.37^{+0.01}_{-0.01}$
	22-Jun.-1998	4.32/155	$2.1^{+0.2}_{-0.1}$	$2.43^{+0.01}_{-0.01}$
	04-May-1999	5.93/155	$2.2^{+0.1}_{-0.1}$	$2.76^{+0.01}_{-0.01}$
	26-Apr.-2000	2.53/155	$1.5^{+0.1}_{-0.1}$	$2.02^{+0.01}_{-0.01}$
	28-Apr.-2000	7.00/155	$1.4^{+0.1}_{-0.1}$	$2.00^{+0.01}_{-0.01}$
	30-Apr.-2000	3.95/155	$1.3^{+0.1}_{-0.1}$	$2.01^{+0.01}_{-0.01}$
	09-May-2000	3.73/155	$1.3^{+0.1}_{-0.1}$	$2.09^{+0.01}_{-0.01}$
RX J1117.1+2014	13-Dec.-1999	1.36/85	$3.0^{+0.4}_{-0.4}$	$2.86^{+0.06}_{-0.06}$
1ES 1218+304	12-Jul.-1999	0.94/95	$2.9^{+0.5}_{-0.5}$	$2.51^{+0.05}_{-0.05}$
1RXS J141756.8+25	13-Jul.-2000	1.12/94	$2.8^{+0.8}_{-0.7}$	$2.23^{+0.06}_{-0.07}$
	23-Jul.-2000	1.16/39	$2.1^{+1.3}_{-1.2}$	$2.22^{+0.15}_{-0.15}$
1ES 1517+656	05-Mar.-1997	1.76/40	$16.3^{+5.8}_{-4.2}$	$2.49^{+0.13}_{-0.13}$
1ES 1553+113	05-Feb.-1998	1.13/68	$6.9^{+3.4}_{-3.4}$	$2.33^{+0.18}_{-0.18}$
Mkn 501	07-Apr.-1997	1.15/236	$1.3^{+0.1}_{-0.1}$	$1.90^{+0.01}_{-0.01}$
	11-Apr.-1997	1.04/233	$0.9^{+0.1}_{-0.1}$	$1.80^{+0.02}_{-0.02}$
	16-Apr.-1997	1.41/236	$0.9^{+0.1}_{-0.1}$	$1.59^{+0.01}_{-0.01}$
	28-Apr.-1998	1.49/147	$1.0^{+0.1}_{-0.1}$	$1.83^{+0.02}_{-0.02}$
	29-Apr.-1998	1.37/142	$1.1^{+0.1}_{-0.1}$	$1.82^{+0.02}_{-0.02}$
	01-May-1998	1.74/144	$1.4^{+0.2}_{-0.1}$	$1.98^{+0.03}_{-0.02}$
	20-Jun.-1998	1.07/147	$1.2^{+0.1}_{-0.1}$	$2.03^{+0.03}_{-0.03}$
	29-Jun.-1998	1.25/147	$1.4^{+0.1}_{-0.1}$	$1.96^{+0.03}_{-0.03}$
	16-Jul.-1998	1.69/147	$1.9^{+0.3}_{-0.1}$	$2.07^{+0.03}_{-0.03}$
	25-Jul.-1998	1.93/147	$1.5^{+0.2}_{-0.1}$	$2.06^{+0.03}_{-0.03}$
	10-Jun.-1999	1.78/147	$1.3^{+0.1}_{-0.1}$	$2.41^{+0.01}_{-0.01}$
H1722+119	24-Aug.-2001	1.29/147	$12.6^{+1.3}_{-1.3}$	$2.56^{+0.02}_{-0.03}$
1ES 1959+650	04-May-1997	1.02/45	$13.3^{+7.5}_{-7.5}$	$2.70^{+0.11}_{-0.11}$
	23-Sep.-2001	1.35/147	$12.5^{+2.1}_{-2.0}$	$2.51^{+0.05}_{-0.05}$
	28-Sep.-2001	1.28/144	$20.9^{+0.9}_{-1.0}$	$2.33^{+0.02}_{-0.01}$
PKS 2005-489	01-Nov.-1998	1.95/145		$2.19^{+0.01}_{-0.01}$
PKS 2155-304	20-Nov.-1996	2.18/231	$1.3^{+0.1}_{-0.1}$	$2.63^{+0.01}_{-0.01}$
	22-Nov.-1997	5.70/147	$2.0^{+0.1}_{-0.1}$	$2.70^{+0.01}_{-0.01}$
	04-Nov.-1999	2.22/147	$0.9^{+0.2}_{-0.1}$	$2.80^{+0.01}_{-0.01}$
1ES 2344+514	03-Dec.-1999	1.41/92	$11.8^{+4.1}_{-3.6}$	$2.33^{+0.04}_{-0.05}$
H2356-309	21-Jun.-1998	1.33/147	$2.1^{+0.4}_{-0.4}$	$2.09^{+0.03}_{-0.04}$
LBLs				
3C 66A	31-Jan.-1999	1.26/35		$2.26^{+0.18}_{-0.17}$
S50716+71	14-Nov.-1996	1.18/49	$0.1^{+0.1}_{-0.1}$	$2.06^{+0.14}_{-0.13}$
	07-Nov.-1998	2.06/35		$2.21^{+0.12}_{-0.14}$
	30-Oct.-2000	1.55/34		$2.05^{+0.13}_{-0.12}$
ON231	11-May-1998	2.86/35		$2.50^{+0.12}_{-0.14}$
	11-Jun.-1998	3.04/34		$2.36^{+0.12}_{-0.14}$
BLLAC	31-Oct.-2000	1.28/147	$10.1^{+2.3}_{-2.3}$	$2.65^{+0.06}_{-0.05}$
FSRQs				
1ES 0836+710	27-May-1998	1.13/147	$78.0^{+54.9}_{-35.2}$	$1.34^{+0.04}_{-0.04}$
3C 273	18-Jul.-1996	1.14/231		$1.58^{+0.01}_{-0.01}$
	24-Jun.-1998	2.22/148		$1.65^{+0.01}_{-0.01}$
	09-Jan.-2000	2.10/148		$1.67^{+0.01}_{-0.01}$
	13-Jun.-2000	1.79/148		$1.68^{+0.01}_{-0.01}$
	12-Jun.-2001	3.08/148		$1.74^{+0.01}_{-0.01}$
PKS 1510-089	03-Aug.-1998	1.37/35		$1.37^{+0.09}_{-0.10}$
PKS 2126-158	24-May-1999	1.06/147	$294.1^{+110.7}_{-86.5}$	$1.62^{+0.04}_{-0.04}$

Columns: 1 = object name; 2 = observation date; 3 = reduced χ^2 and degrees of freedom; 4 = free intrinsic absorption (in units of 10^{20} cm^{-2}); 5 = photon spectral index for the single power law model.